JOC The Journal of Organic Chemistry

Article

pubs.acs.org/joc

β-Oxygen Effect in the Barton−McCombie Deoxygenation Reaction: Further Experimental and Theoretical Findings

Alma Sánchez-Eleuterio, Jacinto Sandoval-Lira, Jenny García-Sánchez, Lorena Monterrosas-Pérez, Julio M. Hernández-Pérez, Leticia Quintero, and Fernando Sartillo-Piscil*

Facultad de Ciencias Químicas, Benemérita Universidad Autónoma de Puebla (BUAP). 14 Sur Esq. San Claudio, San Manuel.72570, Puebla, México

Supporting Information

ABSTRACT: The chemistry of (*S*)-methyl xanthates derived from *xylo*- and *ribo*-furanose derivatives in the presence of the stannyl radical is investigated. Xanthate derived from *β-xylo*-furanose affords exclusively a deoxygenated product; whereas, under the same reaction conditions, the *α-ribo*-furanose xanthate derivative produces quantitatively a hemithioacetal compound. We reasoned that in the case of the *β-xylo*-furanose derivative, a favorable *β*-oxygen effect in the Barton−McCombie deoxygenation reaction is operating where, according to theoretical calculations, unusual molecular orbital interactions (and not strain, as previously proposed) are present. These orbital interactions involve the SOMO (intermediary generated from the stannyl radical addition) with the *σ** orbital of the bond undergoing cleavage and this with the two C−O antibonding orbitals anti oriented. Such molecular orbital interactions are not present in the *α-ribo*-furanose; therefore, the *β*-scission is highly delayed, and due to the reversibly nature of the stannyl radical addition, the *ribo*-furanose xanthate is forced to take an alternative route: the homolytic substitution (S_H2) of the sulfide sulfur by stannyl radical. This radical addition gives the alkoxythiocarbonyl radical, which is trapped by Bu_3SnH before the elimination of carbonyl sulfide; subsequently, radical stannyl addition followed by radical reduction produces the hemithioacetal.

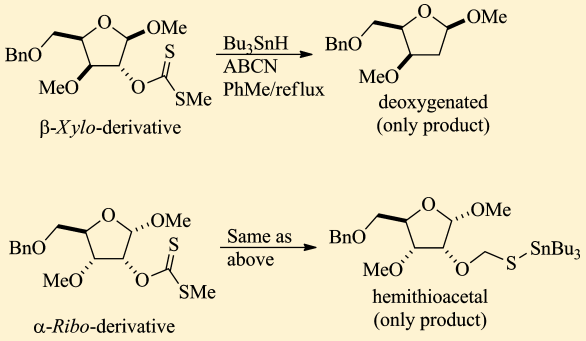

INTRODUCTION

The classic Barton−McCombie reaction is the reaction that transforms secondary alcohols (**1**) into their respective alkane derivatives (**2**) via the temporal transformation of the hydroxyl group into the *O*-methylthiocarbonyl ester (*S*)-methyl xanthate (**3**), followed by a radical hydrogen substitution reaction (Scheme 1).[1] The prevailing reaction mechanism involves the reversible formation of stable carbon-centered radical adduct **A** via stannyl radical addition to the thiocarbonyl group; then, *β*-scission of **A** produces secondary carbon radical **B**, which undergoes reduction by Bu_3SnH (route A, Scheme 1).[1,2] However, an alternative mechanism for the Barton−McCombie reaction has also been postulated: irreversible formation of the alkoxythiocarbonyl radical **C**, which is formed by stannyl radical substitution at the sulfur atom (S_H2), followed by the apparent favorable elimination of carbonyl sulfide to thus produce radical **B** (route B, Scheme 1).[3] Although strong experimental evidence in favor of each mechanism have been provided, competition experiments suggest that deoxygenation via route B represents a less common process.[4]

Scheme 1. Barton−McCombie Reaction

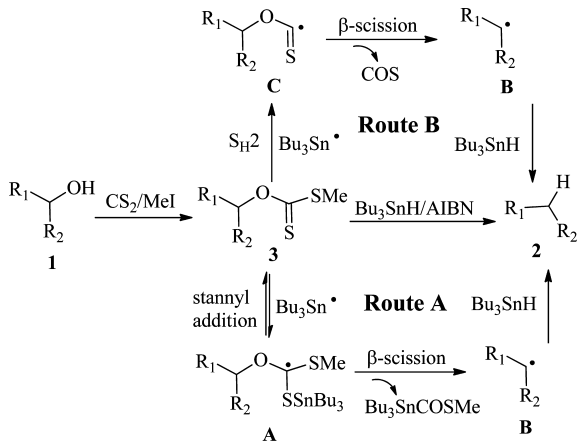

A few years after the invention of this reaction, Barton reported an interesting paper describing a favorable effect on the deoxygenation reaction caused by the presence of an oxygen atom located at the *β*-position to the carbon-centered radical.[5] Actually, it has been commented that the chemistry of the carbon-centered radicals is only perturbed to a minor extent by the presence of either *β*-hydroxy or *β*-alkoxy groups.[6] In this regard, to explain such unusual behavior, Jenkins postulated the existence of polar effects in the *β*-scission step, wherein the thiocarbonyl group and the C−O bond should be antiperiplanar oriented.[7] However, on the basis of electron para-

Received: June 20, 2013
Published: August 29, 2013

   dx.doi.org/10.1021/jo4012943 | J. Org. Chem. 2013, 78, 9127−9136

Scheme 2. Radical Deoxygenation of xylo Furanose (*S*)-Methyl Xanthates 4α and 4β

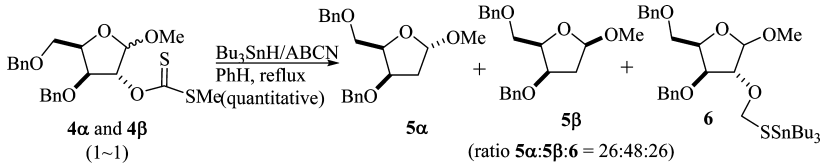

Scheme 3. Preparation of the xylo and ribo Furanose Xanthate Derivatives 10 and 12

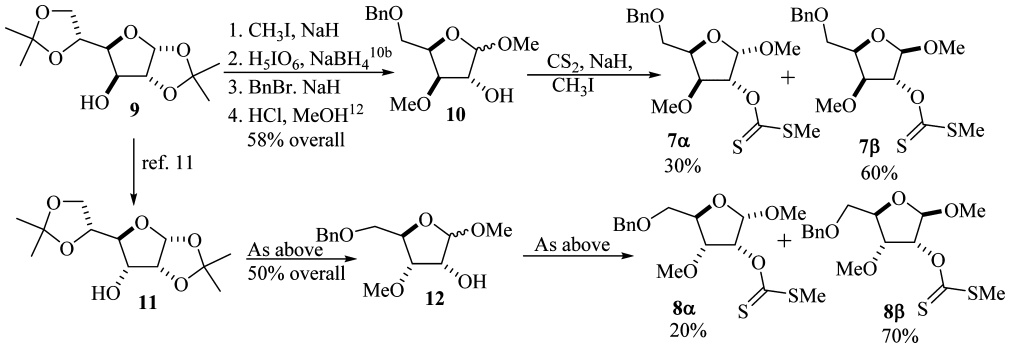

Table 1. Reaction of xylo and ribo Furanose Xanthates 7α, 7β, 8α, and 8β with Stannyl Radical[a]

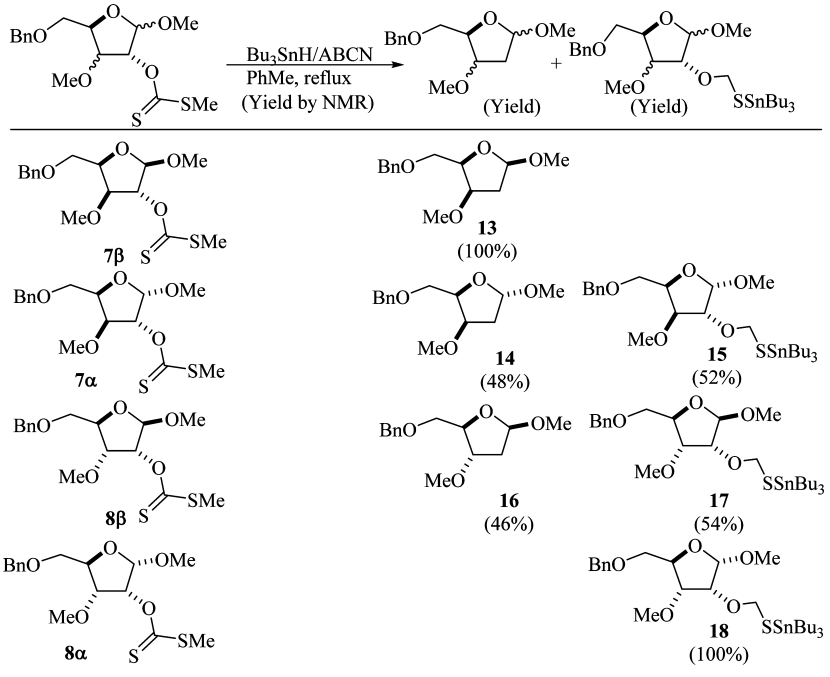

[a]Reactions conducted with 1.8 equiv of Bu_3SnH at 0.068 M.

magnetic resonance (ESR) spectroscopic studies of β-alkoxymethyl radicals, Kochi and Chen stated that the half-filled p orbital is preferentially oriented synclinal to the β-oxygen atom (staggered conformation).[8] Additionally, using competition experiments and computational studies, Crich and Beckwith showed that, in conformationally labile thiocarbonyl esters, the β-scission is not accelerated; however, in conformationally locked analogues, the β-scission is noticeably more rapid, especially when the thiocarbonyl group is axially oriented (i.e., the thiocarbonyl group is oriented synclinal to the β-oxygen atom).[9] They concluded that the main factor of the origin of this β-oxygen effect comes from the greater relief of strain on the β-scission step (steric factors), and the polar effects do not contribute significantly to stabilization of the transition state for the β-scission step. Although all of the explanations concerning the β-oxygen effect in the Barton deoxygenation reaction seem to be satisfactory for each specific situation, it is clear that they do not cover all of the wide range of substrates and reaction conditions. Consequently, further experimental and theoretical studies on this very important topic of free radical chemistry are required.

RESULTS AND DISCUSSION

During the course of a project directed toward the synthesis of biologically active compounds from the chiral pool, we had the need to use the Barton−McCombie deoxygenation reaction to

dx.doi.org/10.1021/jo4012943 | J. Org. Chem. 2013, 78, 9127−9136

Scheme 4. Attempts for Trapping the Putative Radical at C2 and Further Experiments[a]

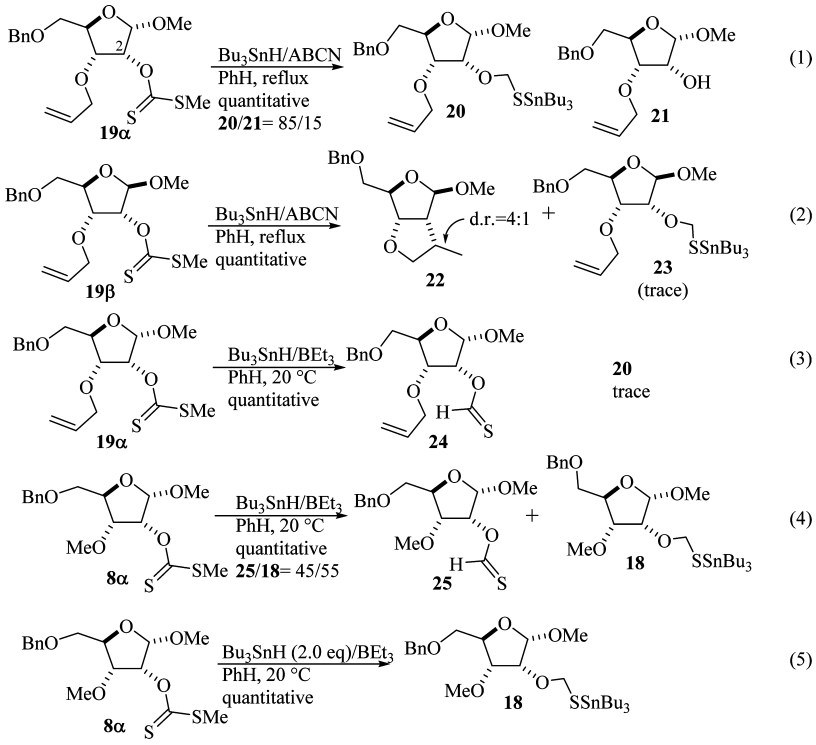

[a]Yields and ratios determined by ^{1}H NMR.

transform the mixture of *α*,*β*-methyl *xylo*-furanose **4** into the respective diastereomeric mixture of tetrahydrofurans **5** (Scheme 2). The mixture of (*S*)-methyl xanthates **4*α*** and **4*β*** was prepared by standard method from their corresponding secondary alcohols.[10] The treatment of the mixture of xanthates **4*α*** and **4*β*** with 1.8 equiv of Bu_3SnH (0.068 M) and 1,1′-azobis-cyclohexanecarbonitrile (ABCN) in refluxing toluene gave two deoxygenated products **5*α*** and **5*β***, and a putative hemithioacetal **6**; and, according to the ^{1}H NMR spectrum, the three products were formed in the ratio 26:48:26, respectively (Scheme 2). It is important to note that purification of the putative hemithioacetal **6** was very difficult due to its inherent instability on silica gel, even neutralizing the silica gel with 2% of NEt_3; in its place, the secondary alcohol precursor of xanthate **4*α*** was obtained. However, the structure of the hemithioacetal product was confirmed with further experimentation (vide infra).

It can be noted from Scheme 2 that complete deoxygenation of the *β*-anomer xanthate (**4*β***) was achieved (**5*β***); however, its *α*-congener was deoxygenated (**5*α***) and transformed into the hemithioacetal **6** in a 1:1 ratio. Intrigued by these unexpected results, we considered it necessary to validate and encompass this observation by preparing a series of (*S*)-methyl *xylo*- and *ribo*-furanose xanthate derivatives **7*α***, **7*β***, **8*α*** and **8*β*** (Scheme 3).

The xanthate precursors **7*α***, **7*β*** and **8*α***, **8*β*** were prepared from alcohols **10** and **12**, respectively,[12] and both alcohols were prepared from the diacetone-D-glucose **9** by using standard methods (Scheme 3).[10−12] The assignment of the stereochemistry of xanthate precursors required chemical correlation of their respective alcohol precursors[12] and two-dimensional nuclear Overhauser effect spectroscopy (2D-NOESY) experiments. It is important to mention that both methoxyl groups, in C1 and C3 positions, were chosen because they would provide similar steric and stereoelectronic demand. And the *ribo*-furanose substrates were chosen because they offer the appropriate stereochemistry to study the apparent relationship between the stereochemistry of the *β*-methoxyl groups on the formation of the hemithioacetal product.

Xylo- and *ribo*-furanose xanthates **7*α***, **7*β***, **8*α***, and **8*β*** were separately treated under the same reaction conditions as the mixture of **4*α***/**4*β***, and according to the reaction crude, the experiments showed complete consumption of starting material to the respective products (Table 1).

Results shown in Table 1 not only validate the initials findings but also set up the strong relation between the stereochemistry of the *β*-C—O bonds and the thiocarbonyl ester on the product ratios. The quantitative isolation of deoxygenation product **13** suggests a beneficial effect in the Barton−McCombie reaction, probably due to the stereoelectronic polar effect, as Jenkins proposed.[7b] Obviously, the synperiplanar relationship between the OMe groups and the thiocarbonyl group in **8*α*** excludes such an effect, and hence the formation of the respective deoxygenated product is much less favored. Although the formation of hemithioacetals from Barton−McCombie reactions have been reported,[2,13] it is important to note that in those cases they are formed as minor byproducts; however, in the present work, the formation of hemithiacetal **18** is the sole observed product. On the basis of these results, we reasoned that the reversible attack of the stannyl radical on the C═S double bond and the lack of the stereoelectronic polar effect in xanthate **8*α*** might be responsible for the formation of the hemithioacetal product **18** (and also for the reaction of **4*α*** → **6**) via the alternative route B shown in Scheme 1. The mixed results for **7*α*** → **14** plus **15**, and **8*β*** → **16** plus **17**, can be taken as additional

dx.doi.org/10.1021/jo4012943 | J. Org. Chem. 2013, 78, 9127−9136

evidence to reinforce all of the just-mentioned. It is important to comment that although all of the reaction crudes were very clear, showing complete consumption of the starting materials and formation of product(s), again, the isolation of the hemithioacetals **15**, **17**, and **18** was quite difficult due to their own instability. However, after a thorough purification either by thin-layer chromatography using benzene as developing solvent or passing the reaction crude through a short column of neutral alumina using hexane as solvent and increasing polarity with ethyl acetate (40:1), sufficient amounts of themithioacetals with acceptable purity for spectroscopic analysis were obtain.

So, why does the alternative route turn into the principal one? And what is the driving force of the exclusive formation of the hemithioacetal product and therefore, the nonformation of the deoxygenated product? Obviously, if we are able to address these questions, we will provide further findings on the origin of the β-oxygen effect in the Barton−McCombie deoxygenation reaction, and in general, in the chemistry of β-alkoxy carbon-centered radicals.

First of all, it was considered reasonable to investigate whether the carbon-centered radical, which should be formed from the β-scission of the adduct radical derived from **8α**, is actually not formed. To this end, thiocarbonyl ester **19α** (and also **19β**) was prepared to trap the putative radical by means of a rapid and favorable 5-exo-trig radical cyclization. The thiocarbonyl esters **19α** and **19β** were prepared from allofuranose **11** following the same route described in Scheme 3. Like xanthate **8α**, the treatment of xanthate **19α** with Bu_3SnH under more diluted conditions afforded thiohemiacetal **20** as the major product and alcohol **21**[14] as the minor product (which comes from hydrolysis of the thiohemicetal **20**), and no trace of the cyclized product (not shown) was detected (eq 1). On the other hand, xanthate **19β** gave the cyclized product **22** as the major product, and thiohemiacetal **23** as the minor product (eq 2). Purification of hemithioacetals **20** and **23** was even more problematic than purification of hemithioacetals **15**, **17**, and **18**; both were only observed by ^{1}H NMR. In particular, the chemical shifts and geminal coupling constants of diastereotopic methylene hydrogen atoms attributable to the hemithioacetal functional group of **20** (δ: 4.92 ppm, ^2J = 10.8 Hz; 4.96 ppm, ^2J = 10.8 Hz) and **23** (δ: 4.92 ppm, ^2J = 10.4 Hz; 4.96 ppm, ^2J = 10.2 Hz) are quite similar to those observed for **14**, **17**, and **18** (δ's in the range 4.84−4.99 ppm and ^2J's in the range 10.2−10.8 Hz).

At this point, it was considered pertinent to varying reactions conditions to xanthates **19α** and **8α** with the expectation to obtain further mechanistic information (Scheme 4). Thus, when xanthate **19α** was reacted with Bu_3SnH (1.5 equiv) and triethylborane at 20 °C, quantitative formation of thioformate **24** was observed, and only a trace of hemithioacetal **20** was detected (eq 3). Similarly, under the same reaction conditions, xanthate **8α** afforded thioformate **25** and hemithiocetal **18** in a 45:55 ratio, respectively (eq 4). And when the amount of Bu_3SnH was increased from 1.5 to 2.0 equiv, the hemithioacetal **18** was exclusively formed (eq 5). Evidently, these experiments not only exclude the formation of carbon-centered radicals at C2 when the two C−O bonds are syn oriented to the thiocarbonyl group but also reinforce the idea of a favorable effect for the formation of the hemithioacetal compounds probably at the expense of an unfavorable β-oxygen effect in the Barton deoxygenation reaction. Furthermore, it appears that at least one C−O bond antiperiplanar oriented to a thiocarbonyl group (**19β** and **8β**) is necessary to trigger the β-scission to thus provide either cyclized product **22** or deoxygenated product **14** (see Table 1 and Scheme 4).

The exclusive formation of the thioformate **24** from **19α** at 20 °C, and the mixture of thioformate **25** and hemithioacetal **18** from **8α** at the same temperature, suggests that hemithioacetals are formed from their respective thioformates via the formation of an alkoxythiocarbonyl radical. The experiment of **8α** to **18** with 2.0 equiv of Bu_3SnH supports this proposal (Scheme 4). It is worth mentioning that, although the presence of alkoxythiocarbonyl radicals has been reported in some Barton−McCombie deoxygenations or similar radical reactions, in the present study, these free radicals are successfully trapped in the form of thioformates demonstrating thus that the elimination of alkoxythiocarbonyl radical is not so simple as previously proposed.[3,15] Additionally, it has been proposed that the formation of hemithioacetals comes from radical adducts of type **E** (e.g., **8α** → **E** → **18**);[2] however, in the present investigation, we provide experimental and theoretical evidence (vide infra) suggesting that hemithioacetals are preferentially formed from thioformates (e.g., **H** → **25** → **18**).[16]

On the basis of these experiments, we are in good position for addressing the above-mentioned questions. The reversible stannyl radical addition on both thiocabonyl groups of **7β** and **8α** at standard conditions should produce radical adducts **D** and **E**, respectively; however, as above-demonstrated, the β-scission to secondary radicals only occurs for the case of **D** → **F** and not for **E** → **G** (Scheme 5).

Scheme 5. Contrasting Behavior of Thioesters 7β and 8α Toward Stannyl Radical

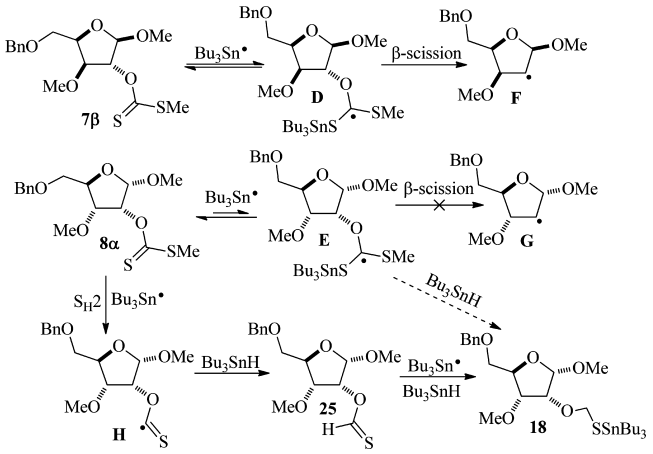

The latter suggests that the equilibrium process between **8α** and adduct radical **E** is driven toward **8α**, forcing it to take a different reaction course: the stannyl radical displacement on the sulfide sulfur atom to form the alkoxythiocarbonyl radical **H**, which is reduced by Bu_3SnH before elimination of carbonyl sulfide. Then, radical stannyl addition followed by radical reduction gives the hemithioacetal **18** (Scheme 5). At first glance, it appears logical to assume that radical **F** should be more stable than radical **G**; however, density functional theory (DFT) calculations performed at B3LYP/6-311+G(d,p) level of theory show that the radical **G** is 2.24 kcal/mol more stable than radical **F**. On the other hand, radical precursor models **L** and **M** show different behavior, radical **L** being 2.95 kcal/mol more stable than radical **M**. These results might be in accordance with the theoretical energies calculated with molecular mechanics by Crich and Beckwith for their

dx.doi.org/10.1021/jo4012943 | J. Org. Chem. 2013, 78, 9127−9136

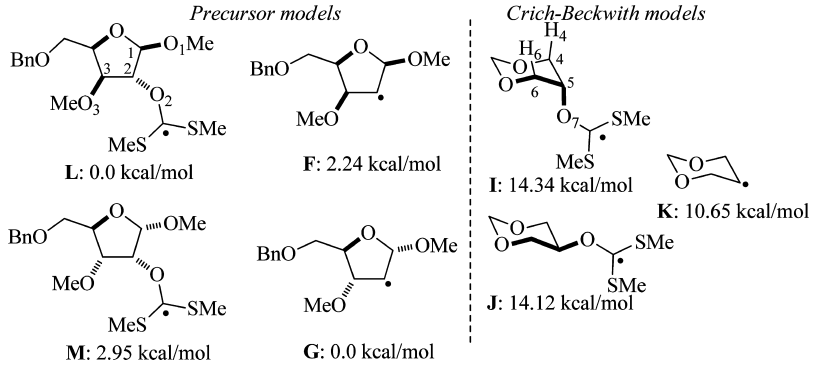

Figure 1. Relative energies of radicals for radical precursor models (**L**, **F**, **M**, and **G**) calculated at B3LYP/6-311+G(d,p) level of theory, and Crich–Beckwith models calculated with Molecular Mechanics (**I**, **J**, and **K**).

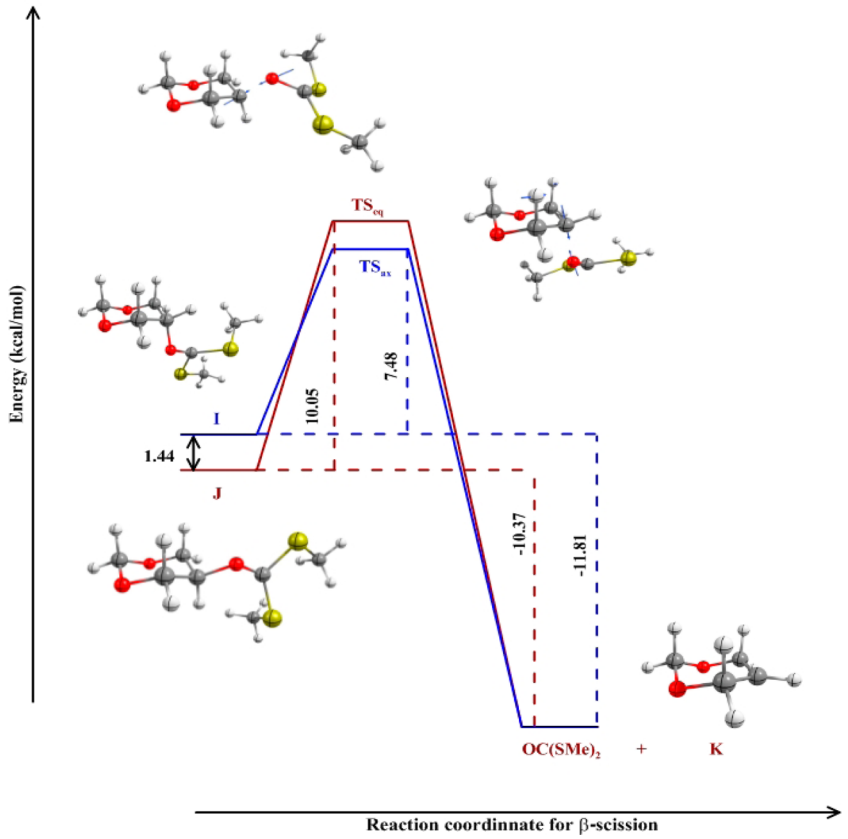

Figure 2. Potential energy surface for the β-scission of **I** → $\mathbf{TS_{ax}}$ → **K** + $\mathbf{OC(SMe)_2}$ and **J** → $\mathbf{TS_{eq}}$→**K** + $\mathbf{OC(SMe)_2}$ calculated at B3LYP/6-311+G(d,p) level of theory.

conformationally semirigid radical model adducts **I** and **J**, wherein the radical adduct derived from the thiocarbonyl ester syn oriented to C–O bond (**I**) is, by only 0.22 kcal/mol, more unstable than the equatorial one (**J**). See Figure 1.

However, in the present study, the differing energies between radical models **L** and **M** cannot be considered as strain energies; otherwise, radical **M** should produce radical **G** more rapidly (as it was interpreted for the case of the radical models **I** and **J**).[9] This suggests that there is something other than simple strain energy in the β-scission. Subsequently, after an investigation into the electronic nature of the Crich–Beckwith radical models **I** and **J**, it was found that the activation energy for the β-scission of **I** is 7.48 kcal/mol, whereas for **J** it is 10.05 kcal/mol; in other words, the transition state $\mathbf{TS_{ax}}$ is 2.57 kcal/mol more stable than $\mathbf{TS_{eq}}$ (Figure 2).

These numbers are more consistent with their experimental results.[9] Additionally, using natural bond orbital (NBO) analysis, it was found that the stabilization energy at the $\mathbf{TS_{ax}}$ transition state comes from the molecular orbital interactions between SOMO and the σ^*_{C5-O7} bond and unusual orbital interaction with two antibonding orbitals[17] σ^*_{C4-H4} and σ^*_{C6-H6} (Table 2). The SOMO → σ^*_{C5-O7} orbital interaction with $E(2)$ = 38.31 kcal/mol and two orbital interactions σ^*_{C5-O7} → σ^*_{C4-H4} and σ^*_{C5-O7} → σ^*_{C6-H6} with $E(2)$ = 0.84 and 0.79 kcal/mol, respectively (see Table 2 and Figure 3).

Having found that interesting and unusual orbital interactions are involved in radical models **I** and **J**, we applied the same computational treatment to radical models **L** and **M**. Surprisingly, model adducts **L** and **M** showed inverse barriers in the activation energy for the β-scission. Now the radical adduct

dx.doi.org/10.1021/jo4012943 | J. Org. Chem. 2013, 78, 9127–9136

Table 2. NBO Analysis (Second-Order Perturbation Theory) of Hyperconjugative Interactions in Structures TS_{ax} and TS1 Calculated at the B3LYP/6-311+G(d,p) Level of Theory

donor orbital	acceptor orbital	$E(2)$ (kcal/mol)	$\varepsilon_i-\varepsilon_j$ (ua)	F_{ij} (ua)
TS_{ax}				
SOMO	σ^*_{C5-O7}	38.31	0.19	0.110
σ^*_{C5-O7}	σ^*_{C4-H4}	0.84	0.37	0.039
σ^*_{C5-O7}	σ^*_{C6-H6}	0.79	0.37	0.039
TS1				
SOMO	σ^*_{C2-O2}	36.47	0.20	0.110
σ^*_{C2-O2}	σ^*_{C1-O1}	1.30	0.32	0.046
σ^*_{C2-O2}	σ^*_{C3-O3}	1.56	0.31	0.051

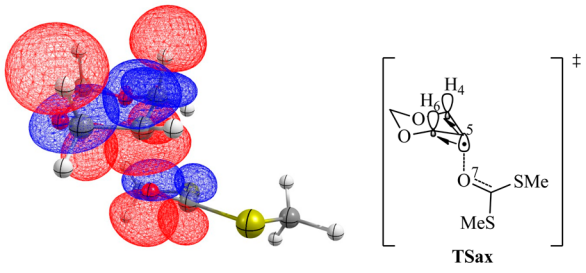

Figure 3. NBO orbital interaction SOMO → σ^*_{C5-O7} and two orbital interactions σ^*_{C5-O7} → σ^*_{C4-H4} and σ^*_{C5-O7} → σ^*_{C6-H6} at the transition state (TS_{ax}).

L, derived from the xanthate that orients the thiocarbonyl ester group anti to C−O bonds, possesses the lower energy barrier for the formation of secondary radical **F** ($\Delta E^{\ddagger}_{L\rightarrow TS1}$ = 9.70 kcal/mol); on the other hand, its radical congener **M** requires considerably more energy for the formation of the secondary radical **G** ($\Delta E^{\ddagger}_{M\rightarrow TS2}$ = 13.28 kcal/mol) (Figure 4). In fact, the latter high barrier is more than enough to destabilize transition state **TS2** and therefore is responsible for the nonformation of the radical **G**. Hence, this high destabilizing energy may explain why the equilibrium between **8*α*** and adduct radical **E**, described in Scheme 5, is driven toward **8*α***, and it also may explain the formation of the hemithioacetal product.

Analyzing electronic transitions states structures **TS1** and **TS2**, we found that the lowering of the transition state energy of **TS1** is due to the same unusual molecular orbital interactions of the SOMO with σ^*_{O2-C2} and two antibonding orbitals σ^*_{C1-O1} and σ^*_{C3-O3}. The remarkably low energy barrier of **TS1** is due to the higher acceptor capacity of the two antibonding orbitals σ^*_{C1-O1} and σ^*_{C3-O3} (compared to those for the two antibonding orbitals σ^*_{C4-H4} and σ^*_{C6-H6} of TS_{ax}). The energy of SOMO → σ^*_{O2-C2} orbital interaction is on the order of $E(2)$ = 36.47 kcal/mol, and two orbital interactions σ^*_{O2-C2} → σ^*_{C1-O1} and σ^*_{O2-C2} → σ^*_{C3-O3} with $E(2)$ energies of 1.37 and 1.56 kcal/mol, respectively (Table 2 and Figure 5). These electronic interactions are not present in the **TS2**.

The energy and occupancy of the antibonding orbitals were calculated to explain this double hyperconjugative interaction (Table 3). The orbital occupancy value for the antibonding orbitals **TSax** and **TS1** are very similar: σ^*_{C5-O7} = 0.283 and σ^*_{C2-O2} = 0.276, indicating that both *β*-scission for radical **I** and radical **L** are quite favorable. The reason for these high occupancy values is due to the interaction energy of the SOMO → σ^*_{C5-O7} in TS_{ax} (38.31 kcal/mol) and the SOMO → σ^*_{C2-O2} in **TS1** (36.47 kcal/mol). Additionally, the NBO analysis revealed that the orbital interactions σ^*_{O2-C2} → σ^*_{C1-O1} and σ^*_{O2-C2} → σ^*_{C3-O3} are more stabilizing than the σ^*_{C5-O7} → σ^*_{C4-H4} and σ^*_{C5-O7} → σ^*_{C6-H6} interactions. Therefore, it can be established that the former interactions are responsible for the favorable *β*-oxygen effect in the Barton−McCombie reaction in the *β-xylo*-furanose xanthate derivatives.

CONCLUSIONS

On the basis of the experimental and theoretical efforts presented herein, we can conclude that the *β*-oxygen effect in the Barton−McCombie reaction is highly favored by unusual orbital interactions between the *σ** orbital of the bond undergoing cleavage with C−O antibonding orbitals placed in *β*-position anti oriented. These orbital interactions lower considerably the transition state energy of the *β*-scission, favoring thus the deoxygenation step; however, when those interactions are not present, the transition state is highly destabilized so the *β*-scission is repressed (or delayed); therefore, the deoxygenation does not proceed. Under this critical scenario and due to the reversibly nature of the first step of the Barton−McCombie reaction (the stannyl addition to thiocarbonyl group), the stannyl radical prefers to attack the SMe group (homolytic displacement: S_H2) to afford the alkoxythiocarbonyl radical, which is trapped by Bu_3SnH and subsequently transformed into the hemithioacetal compound. These results suggest that the alkoxythiocarbonyl radical is formed during the deoxygenation reaction as long as the barrier in the activation energy for the *β*-scission is considerably high, and that the elimination of the carbonyl sulfide is not that easy.[15,17] Probably, similar molecular orbital interactions are necessary to favor the *β*-scission of the alkoxythiocarbonyl radical to thus produce deoxygenation through the alternative route B. Finally, the implications of these findings might be extended to similar carbon-centered free radicals where their behavior is also strongly perturbed by the presence of a *β*C−O bond (i.e., nucleotide C3′,C′4 radical cation).[6,24]

EXPERIMENTAL SECTION

General Information. All reagents purchased commercially were used without purification. The solvents were used as technical grade and freshly distilled prior to use unless otherwise noted. ^{1}H NMR and ^{13}C NMR spectra were recorded with 400 and 100 MHz spectrometers, respectively. ^{1}H NMR and ^{13}C NMR spectra were recorded in $CDCl_3$ and are reported in ppm relative to tetramethylsilane (TMS). Data for ^{1}H NMR are reported as follows: chemical shift (*δ* ppm), multiplicity (s = singlet, d = doublet, t = triplet, q = quartet, m = multiplet), coupling constant (Hz), and integration. Data for ^{13}C NMR are reported in terms of chemical shift. Optical rotations (Na lamp, 589 nm, 20 °C), and $[\alpha]_D$ values are reported in 10^{-1} dg cm^2 g^{-1}; concentration (*c*) is in g/100 mL.

Computational Studies. All calculations were performed using Gaussian 09,[18] and all structures were visualized using the Chemcraft 1.6 program.[19] We carried out the complete set of calculations for the reactions under study with DFT using the B3LYP hybrid functional[20] and Tao, Perdew, Staroverov, and Scuseria (TPSS) meta-generalized gradient approximation (meta-GGA) functional[21] with the 6-311+G(d,p) basis set. All minima and transition state structures were validated by subsequent frequency calculations at the same level of theory. The minimum structures have a set of positive second derivatives, while transition states have one imaginary frequency. The searching of the transition states was conducted by implying the Berny algorithm (opt = TS).[22] Electronic structures of radicals were studied by using NBO analysis, and the stabilizing energies are calculated by second-order perturbation theory analysis.[23] Unrestricted calculations were used for open shell system. No spin contamination was found for radicals; begin the $\langle S^2\rangle$ value about 0.750 in all cases. B3LYP and

dx.doi.org/10.1021/jo4012943 | J. Org. Chem. 2013, 78, 9127−9136

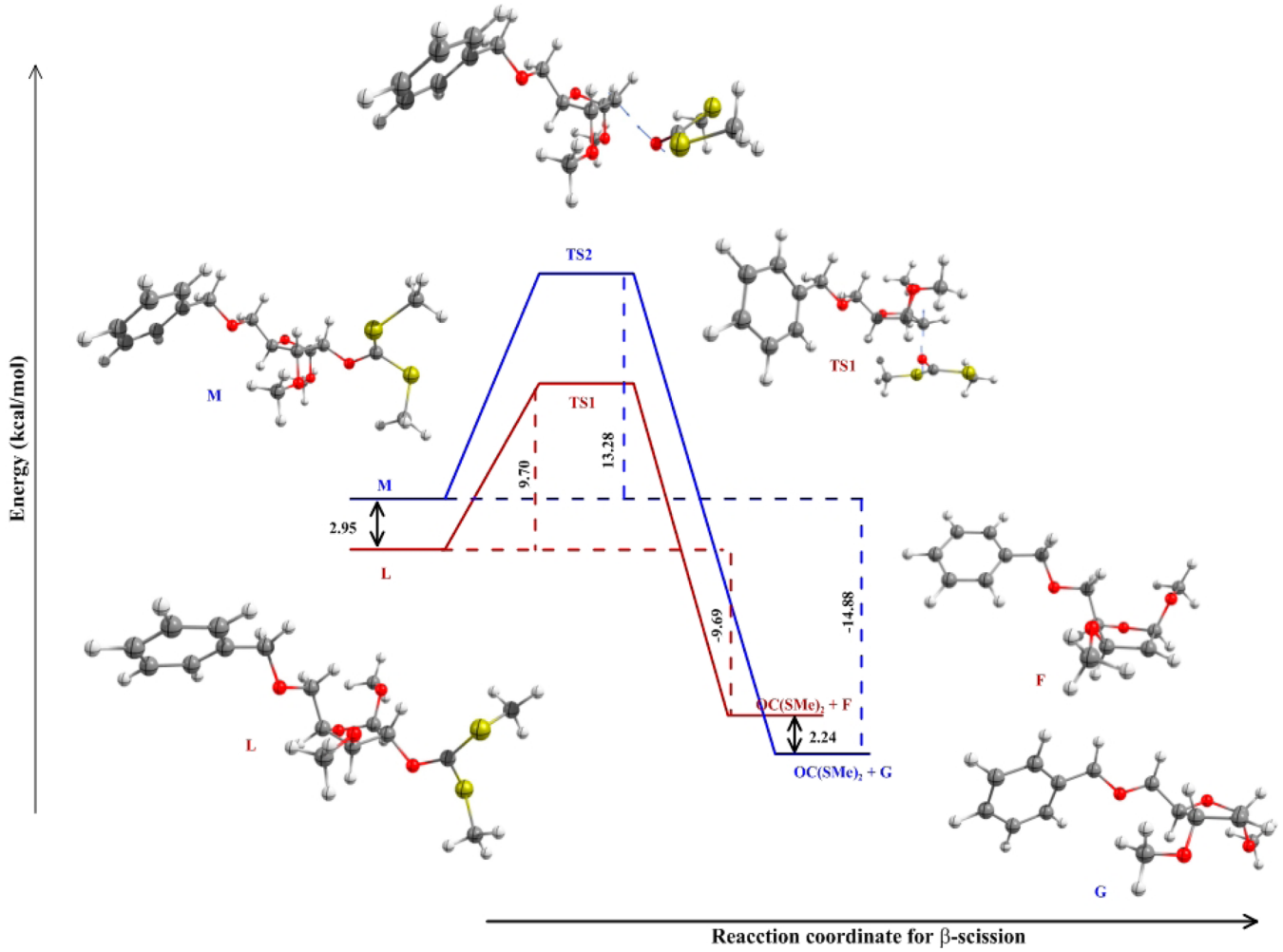

Figure 4. Potential energy surface for the β-scission of **L** → **TS1** → $\mathbf{OC(SMe)_2}$ + **F** and **M** → **TS2** → $\mathbf{OC(SMe)_2}$ + **G** calculated at the B3LYP/6-311+G(d,p) level.

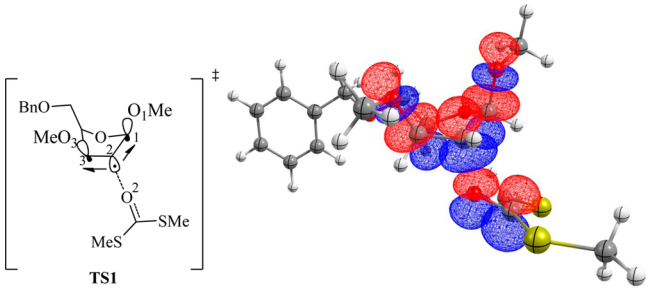

Figure 5. NBO orbital interaction SOMO → σ^*_{O2-C2} and two orbital interactions: σ^*_{O2-C2} → σ^*_{C1-O1} and σ^*_{O2-C2} → σ^*_{C3-O3} at the transition state (**TS1**).

Table 3. NBO Energies and Occupancy for the SOMO Orbital and Antibonding Orbitals Calculated at the B3LYP/6-311+G(d,p) level for structures TS_{ax} and TS1

TS_{ax}			TS1		
orbital	energy (ua)	occupancy	orbital	energy (ua)	occupancy
SOMO	−0.2120	0.758	SOMO	−0.2206	0.752
σ^*_{C5-O7}	−0.2093	0.283	σ^*_{C2-O2}	−0.0185	0.276
σ^*_{C4-H4}	0.3494	0.022	σ^*_{C1-O1}	0.3050	0.040
σ^*_{C6-H6}	0.3534	0.019	σ^*_{C3-O3}	0.2949	0.025

TPSS results show the same trend in all cases. Only discussed results of B3LYP and TPSS results are available in the Supporting Information.

General Procedure for the Formations of Alcohols 10*α*, 10*β*, 12*α*, and 12*β*.[12] 1,2-*O*-Isopropyliden-*α*-D-*xylo*-furanose was dissolved in a solution of HCl (4 mL, 4 N) and MeOH (8 mL) and the solution was heated at refluxing temperature for 1.3 h. After this time, the reaction mixture was treated with a saturated aqueous solution of $NaHCO_3$ (5 mL) and extracted three times with ethyl acetate (30 mL). The organic phase was dried with Na_2SO_4 and evaporated under reduced pressure, and resultant residue was purified by column chromatography on silica gel.

5-O-Benzyl-1,3-O-dimethyl-β-D-ribo-furanose ***12β.*** Purified by column chromatography on silica gel (eluent: hexane/ethyl acetate 4:1), 2.54 g (70%) of **12*β*** was obtained as a yellow oil: $[\alpha]_D^{20}$ = −18.4 (*c* 1.0, $CHCl_3$); ^{1}H NMR (400 MHz, $CDCl_3$) δ 7.38−7.25 (m, 5H), 4.86 (s, 1H), 4.61 (s, 2H), 4.16 (q, *J* = 5.6 Hz, 1H), 4.09 (d, *J* = 4.8 Hz, 1H), 3.86 (dd, *J* = 6.0, 4.8 Hz, 1H), 3.61−3.55 (m, 2H), 3.41 (s, 3H), 3.33 (s, 3H), 2.74 (d, *J* = 3.2 Hz, 1H); ^{13}C NMR (100 MHz, $CDCl_3$) δ 138.1, 128.3, 127.6, 108.5, 81.6, 80.3, 73.2, 72.9, 71.8, 58.4, 55.0; HRMS (FAB-QMS) $[M + H]^+$ calcd for $C_{14}H_{21}O_5$ 269.1389, found 269.1414

5-O-Benzyl-1,3-O-dimethyl-α-D-ribo-furanose ***12α:*** Purified by column chromatography on silica gel (eluent: hexane/ethyl acetate 2:1), 0.72 g (20%) of **12*α*** was obtained as a yellow oil: $[\alpha]_D^{20}$ = +69.2 (*c* 1.0, $CHCl_3$); ^{1}H NMR (400 MHz, $CDCl_3$) δ 7.39−7.31 (m, 5H), 4.88 (d, *J* = 4.7 Hz, 1H), 4.60 (d, *J* = 12.0 Hz, 1H), 4.56 (d, *J* = 12.0 Hz, 1H), 4.19−4.13 (m, 2H), 3.61−3.56 (m, 4H), 3.48 (s, 3H), 3.44

dx.doi.org/10.1021/jo4012943 | J. Org. Chem. 2013, 78, 9127−9136

(s, 3H), 2.87 (d, J = 11.1 Hz, 1H); ^{13}C NMR (100 MHz, $CDCl_3$) δ 138.0, 128.4, 127.7, 127.6, 103.0, 81.7, 79.5, 73.5, 71.9, 70.5, 59.4, 55.9; HRMS (FAB-QMS) $[M + H]^+$ calcd for $C_{14}H_{21}O_5$ 269.1389, found 269.1370

5-O-Benzyl-1,3-O-dimethyl-β-D-xylo-furanose ***10β:*** Purified by column chromatography on silica gel (eluent: hexane/ethyl acetate 4:1), 2.1 g (60%) of **10β** was obtained as a yellow oil: $[\alpha]_D^{20} = -65.5$ (c 1.0, $CHCl_3$); ^{1}H NMR (400 MHz, $CDCl_3$) δ 7.35−7.26 (m, 5H), 4.81(s, 1H), 4.61(d, J = 12.0 Hz, 1H), 4.53 (d, J = 12.0 Hz, 1H), 4.50 (ddd, J = 7.2, 6, 4.8 Hz, 1H), 4.17 (s,1H), 3.74−3.70 (m, 2H), 3.63 (dd, J = 10.4, 7.6 Hz, 1H), 3.39 (s, 1H); ^{13}C NMR (100 MHz, $CDCl_3$) δ 138.2, 128.3, 127.8, 127.6, 109.6, 85.9, 80.2, 78.8, 73.4, 69.6, 58.6, 55.75; HRMS (FAB-QMS) $[M - H]^+$ calcd for $C_{14}H_{19}O_5$ 267.1232, found 267.1258

5-O-Benzyl-1,3-O-dimethyl-α-D-xylo-furanose ***10α.*** Purified by column chromatography on silica gel (eluent: hexane/ethyl acetate 3:1), 1.08 g (30%) of **10α** was obtained as a yellow oil: $[\alpha]_D^{20} = +52.8$ (c 1.0, $CHCl_3$); ^{1}H NMR (400 MHz, $CDCl_3$) δ 7.35−7.33 (m, 5H), 4.97 (d, J = 4.8 Hz, 1H), 4.64 (d, J = 12.0 Hz, 1H), 4.52 (d, J = 12.0 Hz, 1H), 4.38 (ddd, J = 6.8, 6.0, 4 Hz,1H), 4.19 (dt, J = 6, 4 Hz, 1H), 3.76 (dd, J = 6, 4 Hz, 1H), 3.67 (dd, J = 10.8, 4 Hz, 1H), 3.58 (dd, J = 10.8, 7.2 Hz, 1H), 3.49 (s, 3H), 3.40 (s, 3H); ^{13}C NMR (100 MHz, $CDCl_3$) δ 138.2, 128.3, 127.7, 127.5, 101.7, 85.8, 77.3, 76.4, 73.4, 68.8, 57.9, 55.8; HRMS (FAB-QMS) $[M - H]^+$ calcd for $C_{14}H_{19}O_5$ 267.1232, found 267.1210

Xanthates Were Prepared According the Traditional Procedure.[1] *5-O-Benzyl-1,3-O-methyl-2-O-[(methylthio)-thiocarbonyl]-α-D-xylo-furanose* ***7α.*** Purified by column chromatography on silica gel (eluent: hexane/ethyl acetate 20:1), 798 mg (30%) of **7α** was obtained as a yellow oil: $[\alpha]_D^{20} = +103.1$ (c = 1.0, $CHCl_3$); ^{1}H NMR (400 MHz, $CDCl_3$) δ 7.40−7.25 (m, 5H), 5.67 (t, J = 4.8 Hz, 1H), 5.28 (d, J = 4.8 Hz, 1H), 4.65 (d, J = 12.1 Hz, 1H), 4.55 (d, J = 12.2 Hz, 1H), 4.45 (td, J = 6.7, 3.9 Hz, 1H), 4.29 (dd, J = 6.9, 5.4 Hz, 1H), 3.71 (dd, J = 10.7, 4.0 Hz, 1H), 3.62 (dd, J = 10.7, 6.5 Hz, 1H), 3.38 (s, 3H), 3.37 (s, 3H), 2.59 (s, 3H); ^{13}C NMR (100 MHz, $CDCl_3$) δ 215.5, 138.2, 128.3, 127.7, 127.6, 99.7, 85.6, 82.1, 75.9, 73.5, 68.6, 58.3, 55.8, 19.4; HRMS (FAB-QMS) $[M + H]^+$ calcd for $C_{16}H_{23}O_5S_2$ 359.0987, found 359.0952.

5-O-Benzyl-1,3-O-methyl-2-O-[(methylthio)thiocarbonyl]-β-D-xylo-furanose ***7β.*** Purified by column chromatography on silica gel (eluent: hexane/ethyl acetate 15:1), 1.59 g (60%) of **7β** was obtained as a yellow oil: $[\alpha]_D^{25} = -48.7$ (c = 1.0, $CHCl_3$); ^{1}H NMR (400 MHz, $CDCl_3$) δ 7.41−7.22 (m, 5H), 5.84 (s, 1H), 5.04 (s, 1H), 4.63 (d, J = 12.0 Hz, 1H), 4.56 (d, J = 12.0 Hz, 1H), 4.49 (dt, J = 7.2, 5.2 Hz, 1H), 3.93 (d, J = 5.6 Hz, 1H), 3.78 (dd, J = 10.0, 5.2 Hz, 1H), 3.70 (dd, J = 10.0, 7.2 Hz, 1H), 3.47 (s, 3H), 3.42 (s, 3H), 2.57 (s, 3H); ^{13}C NMR (101 MHz, $CDCl_3$) δ 214.4, 138.1, 128.3, 127.8, 127.6, 107.0, 86.9, 82.7, 81.3, 73.4, 69.0, 59.1, 55.9, 19.3; HRMS (FAB-QMS) $[M + H]^+$ calcd for $C_{16}H_{23}O_5S_2$ 359.0987, found 359.0948.

5-O-Benzyl-1,3-O-methyl-2-O-[(methylthio)thiocarbonyl]-α-D-ribo-furanose ***8α.*** Purified by column chromatography on silica gel (eluent: hexane/ethyl acetate 15:1), 532 mg (20%) of **8α** was obtained as a yellow oil: $[\alpha]_D^{20} = +50.0$ (c = 1.0 $CHCl_3$); ^{1}H NMR (400 MHz, $CDCl_3$) δ 7.37−7.26 (m, 5H), 5.65 (dd, J = 7.0, 4.6 Hz, 1H), 5.20 (d, J = 4.8 Hz, 1H), 4.64 (d, J = 12.0 Hz, 1H), 4.56 (d, J = 12.0 Hz, 1H), 4.27 (q, J = 3.8 Hz, 1H), 3.96 (dd, J = 7.0, 4.0 Hz, 1H), 3.64 (m, 2H), 3.46 (s, 3H), 3.38 (s, 3H), 2.60 (s, 3H); ^{13}C NMR (100 MHz, $CDCl_3$) δ 215.8, 137.8, 128.4, 127.7, 127.65, 101.4, 81.7, 79.2, 77.7, 73.5, 69.9, 59.6, 55.8, 19.3; HRMS (EI-QMS) $[M]^+$ calcd for $C_{16}H_{22}O_5S_2$ 358.0909, found 358.0914.

5-O-Benzyl-1,3-O-methyl-2-O-[(methylthio)thiocarbonyl]-β-D-ribo-furanose ***8β.*** Purified by column chromatography on silica gel (eluent: hexane/ethyl acetate 20:1), 1.86 g (70%) of **8β** was obtained as a yellow oil: $[\alpha]_D^{20} = +14.2$ (c = 1.0, $CHCl_3$); ^{1}H NMR (400 MHz, $CDCl_3$) δ 7.41−7.23 (m, 5H), 5.95 (d, J = 4.4 Hz, 1H), 4.99 (s, 1H), 4.65 (d, J = 12.0 Hz, 1H), 4.61 (d, J = 12.0 Hz, 1H), 4.26 (ddd, J = 7.6, 5.6, 3.6 Hz, 1H), 4.06 (dd, J = 7.2, 4.4 Hz, 1H), 3.70 (dd, J = 10.4, 3.6 Hz, 1H), 3.60 (dd, J = 10.4, 6.0 Hz, 1H), 3.37 (s, 3H), 3.35 (s,3H), 2.58 (s, 3H); ^{13}C NMR (100 MHz, $CDCl_3$) δ 215.4, 138.1, 128.3, 127.6, 127.6, 105.6, 81.4, 80.8, 79.8, 73.3, 71.1, 59.0, 55.2, 19.0; HRMS (FAB-QMS) $[M + H]^+$ calcd for $C_{16}H_{23}O_5S_2$ 359.0987, found 359.0977.

3-O-Allyl-5-O-benzyl-1-O-methyl-2-O-[(methylthio)-thiocarbonyl]-α-D-ribo-furanose ***19α.*** Purified by column chromatography on silica gel (eluent: hexane/ethyl acetate 8:1), 625 mg (24%) of **19α** was obtained as a yellow oil: $[\alpha]_D^{20} = +65.8$ (c = 1.0, $CHCl_3$); ^{1}H NMR (400 MHz, $CDCl_3$) δ 7.42−7.21 (m, 5H), 5.85−5.75 (m, 1H), 5.64 (dd, J = 7.2, 4.8 Hz, 1H), 5.20 (d, J = 4.4 Hz, 1H), 5.13 (m, 2H), 4.63(d, J = 12.0 Hz, 1H), 4.53 (d, J = 12.0 Hz, 1H), 4.26 (q, 3.6 Hz, 1H), 4.12−4.071 (m, 2H), 3.94 (dd, J = 13.2, 6.4 Hz, 1H), 3.65 (dd, J = 10.8, 3.6 Hz, 1H), 3.60 (dd, J = 10.8, 4.2 Hz, 1H), 3.45 (s, 3H), 2.60 (s, 3H); ^{13}C NMR (100 MHz, $CDCl_3$) δ 215.7, 137.8, 134.4, 128.3, 127.7, 127.6, 117.6, 101.5, 81.7, 78.9, 74.8, 73.4, 72.4, 69.4, 55.7, 19.2; HRMS (FAB-QMS) $[M + H]^+$ calcd for $C_{18}H_{25}O_5S_2$ 385.1143, found 385.1156.

3-O-Allyl-5-O-benzyl-1-O-methyl-2-O-[(methylthio)-thiocarbonyl]-β-D-ribo--furanose ***19β.*** Purified by column chromatography on silica gel (eluent: hexane/ethyl acetate 15:1), 1.95 g (76%) of **19β** was obtained as a yellow oil: $[\alpha]_D^{20} = +25.2$ (c = 1.0, $CHCl_3$); ^{1}H NMR (400 MHz, $CDCl_3$) δ 7.42−7.21 (m, 5H), 5.92 (d, J = 4.4 Hz, 1H), 5.81 (m, 1H), 5.24 (dm, J = 17.2 Hz, 1H), 5.12 (dm, J = 10.4 Hz, 1H), 5.00 (s, 1H), 4.64 (d, J = 12.0 Hz, 1H), 4.60 (d, J = 12.0 Hz, 1H), 4.28 (ddd, J = 8.0, 6.0, 3.6 Hz, 1H), 4.19 (dd, J = 7.6, 4.0 Hz, 1H), 4.01 (ddt, J = 12.4, 5.6, 1.6 Hz, 1H), 3.94 (ddt, J = 12.4, 4.4, 1.6 Hz, 1H), 3.70 (dd, J = 10.4, 3.6 Hz, 1H), 3.59 (dd, J = 10.4, 6 Hz, 1H), 3.37 (s, 3H), 2.58 (s, 3H); ^{13}C NMR (100 MHz, $CDCl_3$) δ 215.2, 138.3, 133.9, 128.3, 127.6, 117.9, 105.7, 81.7, 80.9, 77.5, 73.3, 72.1, 71.0, 55.2, 18.0; HRMS (FAB-QMS) $[M + H]^+$ calcd for $C_{18}H_{25}O_5S_2$ 385.1143, found 385.1109.

Barton−McCombie Deoxygenation. To a solution of xanthate (100 mg) in dry and degassed benzene (5.0 mL) at 80 °C was added slowly Bu_3SnH (1.8 equiv) and 1,1′-azobis-cyclohexanecarbonitrile (ABCN, 0.5 equiv) dissolved in 1 mL of benzene. The reaction mixture was stirred for 2 h at 80 °C. The resulting mixture was evaporated under reduced pressure and analyzed directly by ^{1}H NMR, and then the residue was purified by column chromatography on silica gel to give the corresponding product. For the case of hemithiocetals, the purification was performed either by thin-layer chromatography using benzene as developing solvent or passing the crude reaction mixture through a short column of neutral alumina using hexane as solvent and increasing polarity with ethyl acetate (40:1). And for the case of thioformates, the tin resides were removed by evaporation of the solvent under reduced pressure followed by liquid−liquid extraction using acetonitrile and hexane. The polar phase (acetonitrile) is evaporated under reduced pressure and the thioformates were characterized by ^{1}H-and ^{13}C NMR.

5-O-Benzyl-2-deoxy-1,3-O-dimethyl-β-D-xylo-furanose ***13.*** Purified by column chromatography on silica gel (eluent: hexane/ethyl acetate 15:1), 67 mg (95%) of **13** was obtained as a yellow oil: $[\alpha]_D^{20} = -85.3$ (c = 1.0, $CHCl_3$); ^{1}H NMR (400 MHz $CDCl_3$) δ 7.40−7.25 (m, 5H), 5.03 (t, J = 3.6 Hz, 1H), 4.63 (d, J = 12.3 Hz, 1H), 4.58 (d, J = 12.3 Hz, 1H), 4.26 (dt, J = 7.5, 5.1 Hz, 1H), 3.92 (m, 1H), 3.78 (dd, J = 10.2, 4.8 Hz, 1H), 3.68 (dd, J = 10.2, 7.5 Hz, 1H), 3.38 (s, 3H), 3.32 (s, 3H), 2.12 (m, 2H); ^{13}C NMR (100 MHz, $CDCl_3$) δ 138.4, 128.3, 127.8, 127.5, 104.9, 81.4, 80.0, 73.4, 69.7, 57.9, 55.6, 37.8; HRMS (FAB-QMS) $[M - H]^+$ calcd for $C_{14}H_{19}O_4$ 251.1283, found 251.1255.

5-O-Benzyl-2-deoxy-1,3-O-dimethyl-α-D-xylo-furanose ***14.*** Thirty-three milligrams (48%) of **14** was obtained as a pale yellow oil: $[\alpha]_D^{25} = +28.8$ (c = 1.0, $CHCl_3$); ^{1}H NMR (400 MHz, $CDCl_3$) δ 7.38−7.30 (m, 3H), 5.13 (dd, J = 5.6, 2.4 Hz, 1H), 4.66 (d, J = 12.2 Hz, 1H), 4.53 (d, J = 12.2 Hz, 1H), 4.23 (dt, J = 6.4, 4.6 Hz, 1H), 3.99 (ddd, J = 6.1, 4.7, 3.0 Hz, 1H), 3.75 (dd, J = 10.4, 4.6 Hz, 1H), 3.66 (dd, J = 10.4, 8.0 Hz, 1H), 3.37 (s, 3H), 3.26 (s, 3H), 2.19 (ddd, J = 14.1, 5.6, 3.0 Hz, 1H), 2.04 (ddd, J = 14.1, 6.4, 2.8 Hz, 1H); ^{13}C NMR (100 MHz, $CDCl_3$) δ 138.3, 128.3, 127.7, 127.5, 104.2, 104.2, 80.5, 79.0, 77.3, 77.0, 76.7, 73.4, 73.3, 68.5, 57.1, 55.3, 55.2, 38.8; HRMS (FAB-QMS) $[M - H]^+$ calcd for $C_{14}H_{19}O_4$ 251.1283, found 251.1259.

5-O-Benzyl-1,3-O-dimethyl-2-O-tributylstannylmethyltio-α-D-xylo-furanose ***15.*** After repeated purifications, 33 mg (20%) of **15** was

dx.doi.org/10.1021/jo4012943 | J. Org. Chem. 2013, 78, 9127−9136

obtained as a pale yellow oil: $[\alpha]_D^{25}$ = +40.2 (*c* = 1.0, $CHCl_3$); ^1H NMR (400 MHz, $CDCl_3$) δ 7.38−7.25 (m, 5H), 4.96 (d, *J* = 10.2 Hz, 1H), 4.94 (d, *J* = 4.4 Hz, 1H), 4.84 (d, *J* = 10.2 Hz, 1H), 4.65 (d, *J* = 12.3 Hz, 1H), 4.53 (d, *J* = 12.0 Hz, 1H), 4.40 (m, 2H), 3.98 (dd, *J* = 6.6, 5.7 Hz, 1H), 3.69 (dd, *J* = 10.5, 4.2 Hz, 1H), 3.58 (dd, *J* = 10.2, 6.9 Hz, 1H), 3.43 (s, 3H), 3.38 (s, 3H), 1.56 (m, 6H), 1.32 (m, 6H), 1.18 (m, 6H), 0.90 (t, *J* = 7.5 Hz, 9H); ^{13}C NMR (100 MHz, $CDCl_3$) δ 138.2, 128.3, 127.7, 127.5, 100.8, 83.6, 79.9, 76.2, 73.4, 69.4, 69.1, 58.7, 55.3, 28.6, 27.0, 13.7; HRMS (FAB-QMS) $[M - H]^+$ calcd for $C_{27}H_{47}O_5SSn$ 603.2166, found 603.2139.

5-O-Benzyl-2-deoxy-1,3-O-dimethyl-β-D-ribo-furanose **16**. Twenty-eight milligrams (40%) of **16** was obtained as a pale yellow oil: $[\alpha]_D^{25}$ = −36.2 (*c* = 1.0, $CHCl_3$); ^1H NMR (400 MHz, CDl_3) δ 7.39−7.24 (m, 5H), 5.08 (dd, *J* = 5.7, 2.4 Hz, 1H), 4.59 (s, 2H), 4.18 (td, *J* = 6.3, 3.6 Hz, 1H), 3.93 (ddd, *J* = 6.9, 5.9, 3.6 Hz, 1H), 3.52 (m, 2H), 3.31 (s, 6H), 2.22 (ddd, *J* = 13.5, 6.9, 2.1 Hz, 1H), 2.06 (m, 1H); ^{13}C NMR (100 MHz, $CDCl_3$) δ 138.2, 128.3, 127.6, 127.6, 105.4, 82.6, 82.0, 73.3, 72.0, 57.2, 55.0, 38.9; HRMS (FAB-QMS) $[M - H]^+$ calcd for $C_{14}H_{19}O_4$ 251.1283, found 251.1260.

5-O-Benzyl-1,3-O-dimethyl-2-O-tributylstannylmethyltio-β-D-ribo-furanose **17**. After repeated purifications, 40 mg (24%) of **17** was obtained as a pale yellow oil: $[\alpha]_D^{25}$ = −25.8 (*c* = 1.0, $CHCl_3$); ^1H NMR (400 MHz, CDl_3) δ 7.38−7.27 (m, 5H), 4.99 (d, *J* = 10.8 Hz, 1H) 4.94 (d, *J* = 10.4 Hz, 1H), 4.93 (s, 1H), 4.60 (m, 2H), 4.29 (d, *J* = 4.8 Hz, 1H), 4.19 (m, 1H), 3.84 (dd, *J* = 6.0, 4.8 Hz, 1H), 3.63 (dd, *J* = 10.4, 3.6 Hz, 1H), 3.55 (dd, *J* = 10.0, 6.4 Hz, 1H), 3.39 (s, 3H), 3.35 (s, 3H), 1.56 (m, 6H), 1.34 (m, 6H), 1.19 (m, 6H), 0.90 (t, *J* = 7.3 Hz, 9H); ^{13}C NMR (100 MHz, $CDCl_3$) δ 138.3, 128.3, 127.6, 127.5, 106.5, 80.9, 80.2, 76.9, 73.2, 71.5, 69.7, 58.3, 55.1, 28.6, 27.0, 13.7, 13.6; HRMS (FAB-QMS) $[M - H]^+$ calcd for $C_{27}H_{47}O_5SSn$ 603.2166, found 603.2186.

5-O-Benzyl-1,3-O-dimethyl-2-O-tributylstannylmethyltio-α-D-ribo-furanose **18**. After repeated purifications, 28 mg (17%) of **18** was obtained as a pale yellow oil: ^1H NMR (400 MHz,CDl_3) δ 7.35−7.27 (m, 5H), 4.95 (d, *J* = 10.8 Hz, 1H), 4.93 (s, 1H) 4.92 (d, *J* = 10.8 Hz, 1H), 4.62 (d, *J* = 12.0 Hz, 1H), 4.56 (d, *J* = 12.0 Hz, 1H), 4.46 (dd, *J* = 6.8, 4.8 Hz, 1H), 4.27 (td, *J* = 4.4, 2.4 Hz, 1H), 3.67 (dd, *J* = 7.2, 2.8 Hz, 1H), 3.60−3.55 (m, 2H), 3.43 (s, 3H), 3.38 (s, 3H), 1.61−1.53 (m, 6H), 1.36−1.30 (m, 6H), 1.21−1.16 (m, 6H), 0.90 (t, *J* = 7.3 Hz, 9H); ^{13}C NMR (100 MHz, $CDCl_3$) δ 137.9, 128.3, 127.5, 127.5, 102.2, 81.9, 78.5, 74.0, 73.4, 70.6, 69.1, 58.7, 55.4, 28.5, 27.0, 13.6; HRMS (FAB-QMS) $[M - H]^+$ calcd for $C_{27}H_{47}O_5SSn$ 603.2166, found 603.2141.

3-O-Allyl-5-O-benzyl-1-O-methyl-α-D-ribo-furanose **21**.[14] Sixty-five milligrams (85.5%) of **21** was obtained as a pale yellow oil: $[\alpha]_D^{25}$ = +119.7 (*c* = 1.0, $CHCl_3$); ^1H NMR (400 MHz, $CDCl_3$) δ 7.37−7.26 (m, 5H), 5.91−5.81(m, 1H), 5.23 (dm, *J* = 17.2 Hz 1H), 5.16 (dm, *J* = 10.4 Hz, 1H), 4.88 (d, *J* = 4.8 Hz, 1H), 4.60 (d, *J* = 12.0 Hz, 1H), 4.52 (d, *J* = 12.0 Hz, 1H), 4.17−4.03 (m, 4H), 3.77 (dd, *J* = 6.8, 2.8 Hz, 1H), 3.56 (d, *J* = 4.0 Hz, 2H), 3.47 (s, 3H), 2.89 (d, *J* = 11.0 Hz, 1H); ^{13}C NMR (100 MHz, $CDCl_3$) δ 137.8, 134.4, 128.4, 127.7, 127.6, 117.7, 102.9, 82.0, 76.5, 73.4, 72.3, 71.7, 70.0, 55.7; HRMS (FAB-QMS) $[M + H]^+$ calcd for $C_{16}H_{23}O_5$ 295.1545, found 295.1570

6-Bencyloxy-melthyl-4-methyloxy-3-methylhexahydrofuro[3,4b]-furan **22**. Purified by column chromatography on silica gel (eluent: hexane/ethyl acetate 8:1), 61 mg (85%) of **22** was obtained as an inseparable diastereoisomerica mixture (4:1). $[\alpha]_D^{25}$ = −33.3 (c = 1.0, $CHCl_3$). NMR data are reported for the major diastereomers: ^1H NMR (400 MHz, $CDCl_3$) δ 7.39−7.26 (m, 5H), 4.94 (d, *J* = 1.7 Hz, 1H), 4.56 (s, 3H), 4.28−4.22 (m, 1H), 3.89 (dd, *J* = 8.4, 6.9 Hz, 1H), 3.56−3.47 (m, 3H), 3.34−3.31 (m, 1H), 3.30 (d, *J* = 0.6 Hz, 3H), 2.74 (ddd, *J* = 8.8, 6.7, 1.6 Hz, 1H), 2.45−2.36 (m, 1H), 1.09 (dd, *J* = 6.9, 2.8 Hz, 3H); ^{13}C NMR (100 MHz, $CDCl_3$) δ 138.1, 128.3, 127.6, 127.6, 106.3, 85.4, 85.2, 74.0, 73.2, 71.6, 54.9, 53.5, 35.4, 12.1; HRMS (FAB-QMS) $[M - H]^+$ calcd for $C_{16}H_{21}O_4$ 277.1440, found 277.1468

Reaction of the Xanthate 8α in the Presence of Triethylborane. To a solution of xanthate **8α** (0.100 g, 0.278 mmol) dissolved in 6 mL of benzene was added BEt_3 (0.139 mL of 1 M solution, 0.139 mmol) at 20 °C. The reaction mixture was stirred for 5 min followed by the slow addition of Bu_3SnH (0.111 mL, 0.417 mmol). The reaction mixture was allowed to stir for 1.3 h and then concentrated under reduced pressure. Analysis of the ^1H NMR spectra revealed clean formation of **25** and **18** in a 45:55 ratio, respectively. For the case of xanthate **19α**, thioformate **24** was observed as the sole product. Unfortunately, all the efforts for purification the thioformates **25** and **24** on silica gel were unsuccessful; the hydrolysis of the thioformate group occurred, and the alcohol precursors of their corresponding xanthates (**8α** and **19α**) were obtained. Furthermore, the stannyl impurities were efficiently removed by dissolving the reaction crude with acetonitrile and extraction with hexane. Thus, thioformates **24** and **25** were obtained with moderate purity.

5-O-Benzyl-1,3-di-O-methyl-2-thioformyl-α-D-ribo-furanose **25**. Twenty-five milligrams (29%) was obtained as a pale yellow oil. $[\alpha]_D^{25}$ = +32.6 (*c* 1.0, $CHCl_3$). NMR data are reported as a rotamer mixture: ^1H NMR (400 MHz, $CDCl_3$) δ 9.75 (s), 8.16 (s), 7.35−7.27 (m), 5.55 (ddd, *J* = 6.0, 4.4, 1.2 Hz), 5.23 (d, *J* = 4.4 Hz), 5.14 (d, *J* = 4.4 Hz), 4.98 (ddd, *J* = 5.6, 4.8, 1.2 Hz), 4.64−4.54 (m), 4.30 (q, *J* = 4.0 Hz), 4.24 (q, *J* = 4.0 Hz), 4.01 (dd, *J* = 6.8, 3.2 Hz), 3.89 (dd, *J* = 6.8, 3.2 Hz), 3.62−3.55 (m), 3.46 (s), 3.45 (s), 3.37 (s), 3.35 (s); ^{13}C NMR (100 MHz, $CDCl_3$) δ 205.5, 160.1, 137.9, 137.7, 128.4, 127.8, 127.6, 101.6, 101.2, 81.8, 81.4, 77.9, 73.6, 72.0, 70.1, 70.0, 59.5, 59.2, 55.7.

5-O-Benzyl-3-O-allyl-1-O-methyl-2-O-thioformyl-α-D-ribo-furanose **24**. Thirty milligrams (34%) yield was obtained as a pale yellow oil. $[\alpha]_D^{25}$ = +29.1 (c = 1.0, $CHCl_3$). NMR data are reported as a rotamer mixture: ^1H NMR (400 MHz, $CDCl_3$) δ 9.75 (s), 8.16 (s), 7.35 (m), 5.82 (m), 5.57 (m) 5.23 (m), 5.17−5.10 (m), 5.01 (m), 4.64−4.52 (m), 4.28 (q, *J* = 3.6 Hz), 4.23 (q, *J* = 4.0 Hz), 4.17 (dd, *J* = 7.2, 3.6 Hz), 4.10−4.02 (m), 3.97 (m) 3.63−3.53 (m), 3.47 (s, 3H), 3.46 (s, 3H); ^{13}C NMR (100 MHz, $CDCl_3$) δ 205.6, 160.06, 137.8, 134.4, 128.4, 127.8, 127.7, 118.0, 117.9, 101.6, 101.3, 82.1, 81.6, 76.2, 75.07, 74.6, 73.5, 72.6, 72.4, 71.7, 69.5, 69.4, 55.7, 28.6, 27.0, 13.6, 13.01.

■ ASSOCIATED CONTENT

Ⓢ Supporting Information

NMR copies for new compounds, calculated energies and thermodynamic parameters for all optimized structures, structure XYZ coordinates for molecules, optimized structure for all transition states, and activation energy diagram for the β-scission calculated at TPSS/6-311+G(d,p) level of theory for key radical models are provided. This material is available free of charge via the Internet at http://pubs.acs.org.

■ AUTHOR INFORMATION

Corresponding Author

*F. Sartillo-Piscil. Tel.:+52 222 2955500 ext. 7391. Fax: + 52 222 2454972. E-mail: fernando.sartillo@correo.buap.mx.

Notes

The authors declare no competing financial interest.

■ ACKNOWLEDGMENTS

We gratefully acknowledge financial support from CONACyT (CB-2012/179074) and the Benemérita Universidad Autónoma de Puebla (BUAP-VIEP).

■ REFERENCES

(1) Barton, D. H. R.; McCombie, S. W. *J. Chem. Soc., Perkin Trans. 1* **1975**, 1574.

(2) See an excellent recent review: McCombie, S. W.; Motherwell, W. B.; Tozer, M. J. *Org. React.* **2011**, 161−432. Also see: Crich, D.; Quintero, L. *Chem. Rev.* **1989**, *89*, 1413.

(3) Barker, P. J.; Beckwith, A. L. J. *J. Chem. Soc., Chem. Commun.* **1984**, 683.

(4) (a) Barton, D. H. R.; Crich, D.; Löbberding, A.; Zard, S. Z. *J. Chem. Soc., Chem. Commun.* **1985**, 646. (b) Barton, D. H. R.; Crich, D.; Löbberding, A.; Zard, S. Z. *Tetrahedron* **1985**, *42*, 2329.
(5) Barton, D. H. R.; Hartwig, W.; Motherwell, W. B. *J. Chem. Soc., Chem. Commun.* **1982**, 447.
(6) Crich, D.; Mo, X.-S. *J. Am. Chem. Soc.* **1997**, *119*, 249.
(7) (a) Quiclet-Sire, B.; Zard, S. Z. *J. Am. Chem. Soc.* **1996**, *118*, 9190. (b) Jenkins, I. D. *J. Chem. Soc., Chem. Commun.* **1994**, 1227 And reference cited therein..
(8) Chen, K. S.; Kochi, J. K. *J. Am. Chem.* **1974**, *94*, 1383. Also see: Beckwith, A. L. J. *Chem. Soc. Rev.* **1993**, *22*, 143.
(9) Crich, D.; Beckwith, A. L. J.; Chen, C.; Yao, Q.; Davinson, I. G. E.; Longmore, R. W.; Anaya de Parrodi, C.; Quintero-Cortés, L.; Sandoval-Ramirez, J. *J. Am. Chem. Soc.* **1995**, *117*, 8757.
(10) (a) Dyatkina, N. B.; Azhayev, A. V. *Synthesis* **1984**, 961. (b) Xie, M.; Berges, D. A.; Robins, M. J. *J. Org. Chem.* **1996**, *61*, 5178.
(11) Cruz-Gregorio, S.; Hernández, L.; Vargas, M.; Quintero, L.; Sartillo-Piscil, F. *J. Mex. Chem. Soc.* **2005**, *49*, 20.
(12) Kovac, P.; Petrikova, M. *Carbohydr. Res.* **1971**, *19*, 249.
(13) Zard, S. Z. In *Handbook of Raft Polymerization*; Barner-Kowollik, C., Ed.; Wiley-VCH: Weinheim, Germany, 2008.
(14) Desai, T.; Gigg, J.; Gigg, R. *Carbohydr. Res.* **1996**, *280*, 209.
(15) (a) Forbes, E. J.; Zard, S. Z. *Tetrahedron Lett.* **1989**, *30*, 4367. (b) Forbes, J.; Zard, S. Z. *Tetrahedron* **1993**, *49*, 825. (c) Coote, M. L.; Easton, C. J.; Zard, S. Z. *J. Org. Chem.* **2006**, *71*, 4996.
(16) Martins, R. C.; Rittner, R.; Tormena, F. C. *J. Mol. Struct. (Theochem.)* **2005**, *728*, 79.
(17) Barton, D. H. R.; Crich, D.; Lobberding, A.; Zard, S. Z. *Tetrahedron* **1986**, *2*, 2329.
(18) Frisch, M. J.; Trucks, G. W.; Schlegel, H. B.; Scuseria, G. E.; Robb, M. A.; Cheeseman, J. R.; Scalmani, G.; Barone, V.; Mennucci, B.; Petersson, G. A.; Nakatsuji, H.; Caricato, M.; Li, X.; Hratchian, H. P.; Izmaylov, A. F.; Bloino, J.; Zheng, G.; Sonnenberg, J. L.; Hada, M.; Ehara, M.; Toyota, K.; Fukuda, R.; Hasegawa, J.; Ishida, M.; Nakajima, T.; Honda, Y.; Kitao, O.; Nakai, H.; Vreven, T.; Montgomery, J. A., Jr.; Peralta, J. E.; Ogliaro, F.; Bearpark, M.; Heyd, J. J.; Brothers, E.; Kudin, K. N.; Staroverov, V. N.; Kobayashi, R.; Normand, J.; Raghavachari, K.; Rendell, A.; Burant, J. C.; Iyengar, S. S.; Tomasi, J.; Cossi, M.; Rega, N.; Millam, J. M.; Klene, M.; Knox, J. E.; Cross, J. B.; Bakken, V.; Adamo, C.; Jaramillo, J.; Gomperts, R.; Stratmann, R. E.; Yazyev, O.; Austin, A. J.; Cammi, R.; Pomelli, C.; Ochterski, J. W.; Martin, R. L.; Morokuma, K.; Zakrzewski, V. G.; Voth, G. A.; Salvador, P.; Dannenberg, J. J.; Dapprich, S.; Daniels, A. D.; Farkas, Ö.; Foresman, J. B.; Ortiz, J. V.; Cioslowski, J.; Fox, D. J. *Gaussian 09*, Revision B.01; Gaussian, Inc.: Wallingford, CT, 2009.
(19) Zhurko, G. A.; Zhurko, D. A. ChemCraft. http://www.chemcraftprog.com
(20) (a) Becke, A. D. *J. Chem. Phys.* **1993**, *98*, 1372. (b) Lee, C.; Yang, W.; Parr, R. G. *Phys. Rev. B.* **1988**, *37*, 785.
(21) Tao, J. M.; Perdew, J. P.; Staroverov, V. N.; Scuseria, G. E. *Phys. Rev. Lett.* **2003**, *91*, 146401.
(22) Peng, C.; Ayala, P. Y.; Schlegel, H. B.; Frisch, M. J. *J. Comput. Chem.* **1996**, *17*, 49.
(23) (a) Foster, P.; Weinhold, F. *J. Am. Chem. Soc.* **1980**, *102*, 7211. (b) Reed, A. E.; Weinhold, F. *J. Chem. Phys.* **1983**, 4066. (c) Reed, A. E.; Weihstock, R. B.; Weinhold, F. *J. Chem. Phys.* **1985**, *83*, 735. (d) Reed, A. E.; Weinhold, F. *J. Chem. Phys.* **1985**, *83*, 1736. (e) Reed, A. E.; Currtis, L. A.; Weinhold, F. *Chem. Rev.* **1988**, *88*, 899.
(24) Crich, D.; Huang, W. *J. Am. Chem. Soc.* **2001**, *123*, 9239.